431

Copy
RM L57G10

NACA RM L57G10

NACA CASE FILE COPY

RESEARCH MEMORANDUM

COMPARISON OF LOW-LIFT DRAG AT MACH NUMBERS FROM 0.74 TO 1.37 OF ROCKET-BOOSTED MODELS HAVING EXTERNALLY BRACED WINGS AND CANTILEVER WINGS

By Waldo L. Dickens and Earl C. Hastings, Jr.

Langley Aeronautical Laboratory
Langley Field, Va.

CLASSIFICATION CHANGED TO UNCLASSIFIED
AUTHORITY: NASA TECHNICAL PUBLICATIONS ANNOUNCEMENTS NO. 11
EFFECTIVE DATE: DECEMBER 1, 1959 WHL

CLASSIFIED DOCUMENT

This material contains information affecting the National Defense of the United States within the meaning of the espionage laws, Title 18, U.S.C., Secs. 793 and 794, the transmission or revelation of which in any manner to an unauthorized person is prohibited by law.

NATIONAL ADVISORY COMMITTEE
FOR AERONAUTICS

WASHINGTON

September 25, 1957

NATIONAL ADVISORY COMMITTEE FOR AERONAUTICS

RESEARCH MEMORANDUM

COMPARISON OF LOW-LIFT DRAG AT MACH NUMBERS FROM 0.74 TO 1.37 OF ROCKET-BOOSTED MODELS HAVING EXTERNALLY BRACED WINGS AND CANTILEVER WINGS

By Waldo L. Dickens and Earl C. Hastings, Jr.

SUMMARY

An investigation has been conducted to determine whether the low-lift drag of a rocket-model airplane-like configuration could be reduced at transonic and low supersonic Mach numbers by reducing the wing thickness while external braces were used to provide the necessary bending strength. The investigation consisted of flight testing two rocket models having aspect ratio 3.04, unswept braced tapered wings mounted on fuselages with the same fineness ratios and cross-sectional area distributions. Data collected from the flight test of a model having a thicker cantilever wing of the same plan form were compared with data collected in this investigation.

The results of this investigation indicated that a wing with a root-mean-square-thickness ratio of 0.0178 with external braces above and below the wing had lower values of drag at transonic and low supersonic Mach numbers than a 4.50-percent-thick cantilever wing. Further reductions in drag and a delayed drag rise Mach number resulted when the 1.78-percent-thick wing was mounted high on a rectangular cross-section body and was externally braced only below the wing.

The investigation also indicated that neither of the externally braced 1.78-percent-thick wings fluttered in the test Mach number range from 0.74 to 1.37.

INTRODUCTION

It is desirable, from the standpoint of minimum drag at transonic and low supersonic speeds, to use wings which are as thin as possible.

The thickness of the wing, however, is usually limited by structural considerations such as its ability to carry bending loads and resist flutter and twisting. A research program has been conducted by the Langley Pilotless Aircraft Research Division to determine the low-lift drag of two rocket-boosted airplane-like configurations having very thin wings with different external bracing arrangements to supply resistance to bending and flutter. Estimates had indicated that the reduction in supersonic pressure drag resulting from a reduction in wing thickness would be considerably greater than the drag increase due to the external braces. The two rocket-boosted models used in this investigation were tested to determine experimentally if this net-drag reduction could be achieved.

This paper presents a comparison of the low-lift drag of a 4.50-percent-thick cantilever wing from reference 1 with that of a 1.78-percent-thick symmetrically, externally braced wing and a 1.78-percent-thick wing with external braces on the bottom surface only between Mach numbers of 0.74 and 1.37. All tests were conducted at the Langley Pilotless Aircraft Research Station at Wallops Island, Va.

SYMBOLS

A	cross-sectional area, sq in.
a_l/g	longitudinal accelerometer reading
C_X	axial-force coefficient, positive in rearward direction
C_D	total drag coefficient based on S
g	acceleration due to gravity, ft/sec^2
γ	flight-path angle, deg
l	length, in.
M	Mach number
q	dynamic pressure, lb/sq ft
R	Reynolds number, based on length of mean aerodynamic chord
S	total wing plan-form area, sq ft
t	time, sec

V velocity along flight path, ft/sec

W weight without propellant, lb

x station measured from nose, in.

MODELS AND FLIGHT TESTS

The bodies of all three models had the same axial distribution of cross-sectional area and each model had a tapered wing of aspect ratio 3.04 which was unswept at the 74.5-percent chord line. The wings were mounted with their vertex at the 49-percent body-length station. Two vertical fins were located at the rear of each body and both the wings and fins had modified hexagonal airfoil sections. Each model fuselage was built around a central structure used to house an internal rocket motor. The wings and fins were attached to this structure and the external fuselage surfaces were of wood.

The wing of model 1 had a 4.50-percent-thickness ratio which was constant from root to tip and was cantilever supported on the fuselage center line. This model was instrumented to obtain base drag and longitudinal acceleration. Table I presents the body coordinates of this model. A three-view drawing and a photograph of the model are presented in figures 1 and 2.

Model 2 was a one-half scale duplicate of model 1 but used a thin wing with external braces above and below the wing. The wing thickness was 1.30 percent at the root, 2.00 percent at the 60-percent semispan, and from this station outboard to the tip the thickness was constant at 2.00 percent. Due to the variation of thickness with span, the root-mean-square value of 0.0178 will be used when discussing the wing thickness throughout this paper. Eight braces symmetrically mounted were used above and below the wing to supply the necessary bending strength. These braces had 6.25-percent-thick modified hexagonal airfoil sections with wedge angles of 12° and were fabricated from 0.0625-inch-thick normalized steel. External steel pylons on the top and bottom of the fuselage and streamlined pods running chordwise across the wing at about the 60-percent semispan were used for attaching the braces to the body and wing. The body coordinates are given in table II and a three-view drawing and photographs are presented as figures 3 and 4. Model 2 was instrumented with a vibrometer in the wing to indicate the existence of flutter.

A three-view drawing of model 3 is shown in figure 5, and figure 6 is a photograph of the model. The physical characteristics are also given on figure 5. Because of the vertical location of the wing above

the body center line (to reduce the amount of external bracing required) a portion of the body had a rectangular rather than circular cross section to reduce the wing-body interference effects. The coordinates of the body are presented in table II.

As was the case with model 2, the root-mean-square thickness ratio of the wing of model 3 was 0.0178 and the plan form was identical to that of both models 1 and 2. External braces were used only below the wing and were mounted between the wing pods and the fuselage itself (eliminating the external mounting pylons). Since the external bracing was all below the wing it was necessary that the braces should always be in tension. This was done by prestressing the braces by making them hold the wing in a bowed position which resulted in a negative dihedral angle of 7.5° at the tip as is shown in figure 5. Model 3 was instrumented to determine wing flutter and measure longitudinal acceleration.

Figures 7(a), 7(b), and 7(c) show the nondimensional cross-sectional area distributions of models 1, 2, and 3, respectively. These figures show that the nondimensional area distribution of the bodies and vertical tails of all the models were the same. The reduction in cross-sectional area due to using the thinner wing (even with the addition of braces, pylons, and pods) is evident by comparing figures 7(b) and 7(c) with the original configuration in 7(a).

A photograph of a typical model-booster combination is shown as figure 8. The first-stage external rocket motor separated from the model at burnout and after a short coasting period the internal rocket motor fired, propelling the model to the desired altitude and Mach number. All of the drag data presented in this paper were obtained after the burnout of the internal rocket motor while the models were coasting at, or near, zero lift between Mach numbers of about 0.7 and 1.6.

During the flight tests the models were tracked by an NACA modified radar tracking unit to determine position in space and by a CW Doppler radar set to determine velocity. A rawinsonde released at the time of firing recorded free-stream temperature, static pressure, and winds aloft.

REDUCTION OF DATA

The velocity of the models, determined from the CW Doppler tracking radar, was used to compute the total drag coefficient by differentiating this velocity with time and correcting for the flight-path angle by the use of the following relationship

$$C_D = -\left(\frac{dV}{dt} + g \sin \gamma\right)\frac{W}{qSg}$$

Reference 2 discusses this method of drag reduction in more detail.

Since models 1 and 3 were instrumented with longitudinal accelerometers, an additional source of drag data was available for the models. The telemetered longitudinal accelerometer values were used to compute the axial-force coefficient by the relationship

$$C_X = \left(-\frac{a_l}{g}\right)\frac{W}{qS}$$

and since these models flew at, or near, zero lift the values of C_X determined were assumed to be numerically equal to C_D.

Mach number was determined by using the radar values of model velocity and the local velocity of sound from rawinsonde measurements of the atmospheric temperature.

ACCURACY

The best method of determining the accuracy of C_D from flight data, when possible, is by a comparison of the values derived from the telemeter and tracking radar. In reference 1 (where the drag data points from the test of model 1 are presented) agreement is shown to be within ±0.0005 between Mach numbers of 0.70 and 1.55 for the test of model 1. A comparison of the two sources of C_D values for model 3 shows agreement within ±0.0005 between Mach numbers of 1.22 and 1.33. In general, these comparisons and other tests of this type indicate that the accuracy of the C_D values presented in this paper should be better than ±0.0010 at Mach numbers near 0.70 and about ±0.0005 at a Mach number of 1.35. Based on the accuracy of the CW Doppler radar set for measuring velocity, the accuracy of M is ±0.005 at $M = 1.35$ and ±0.010 at $M = 0.70$.

RESULTS AND DISCUSSION

Figure 9 presents the variation of Reynolds number R (based on the length of each mean aerodynamic chord) with Mach number for the three models tested and values of total drag coefficient C_D for the three models are presented in figure 10. The drag curve for model 1 is reproduced without data points from reference 1. No values of C_D were obtained in the test of model 2 at Mach numbers less than 0.98. The data points from the test of model 3 are presented in figure 10 to show the agreement between C_D from the telemeter data and the Doppler tracking radar in the Mach number range from 1.22 to 1.33.

Drag comparisons made in this section are presented on the basis of total drag coefficient. The bases of models 2 and 3 were identical and the base of model 1 was geometrically the same as for models 2 and 3. Therefore any differences in C_D due to differences in base configurations were considered negligible.

Figure 9 shows lower test values of R for models 2 and 3 than for model 1. Estimates made to determine this effect on the skin-friction drag of the wing-body combinations for a fully turbulent boundary layer indicated the increase in drag coefficient for models 2 and 3 to be a constant of 0.0013 between $M = 0.70$ and $M = 0.95$, and 0.0008 at $M = 1.40$. A comparison of C_D of models 1 and 3 (fig. 10) between $M = 0.74$ and 0.90 shows that C_D for model 3 is about 0.0015 greater than model 1. Since the difference in drag coefficient is almost entirely a Reynolds number effect between $M = 0.74$ and $M = 0.90$, the influence of the external bracing on C_D is small in this Mach number range.

Between $M = 0.98$ and 1.37 model 2 has lower values of C_D than model 1. At $M = 1.03$ this reduction amounts to about 0.006 (17 percent) and at $M = 1.37$ the difference is 0.002 (7 percent). Model 3 shows lower total-drag values than either model 1 or 2 between $M = 0.98$ and 1.37 and a later drag rise Mach number than model 1. At $M = 1.05$, C_D for model 3 is 0.011 lower than model 1 (about 31 percent) and at $M = 1.39$ is 0.004 lower (about 15 percent).

Also presented in figure 10 is the drag of the wingless body of model 1 (including drag of two fins and base drag) as determined from data presented in reference 1. An estimate of the drag reductions for models 2 and 3 due to reducing the wing thickness was made at $M = 1.10$ by assuming that the pressure drag rise of their wingless bodies (which had the same area distribution) was the same as that for model 1. By using the results of reference 3 (which show that at this Mach number the wing pressure drag is proportional to the wing thickness ratio to approximately the 1.5 power) the reduction in C_D for models 2 and 3 with the unbraced thin wing was estimated to be 0.012 at $M = 1.10$. The measured reduction due to thinning the wing and adding braces was 0.006 for model 2 and 0.008 for model 3. It is evident that although large reductions in C_D for models 2 and 3 were achieved, these reductions are not as large as that estimated for the thin unbraced wing configuration.

The data presented in figure 10 also indicate that at $M = 1.03$ the wing plus brace and interference drag coefficients of models 2 and 3 are lower than the wing plus interference drag of model 1 by about 27 percent and 50 percent, respectively. These reductions decrease with increasing Mach number until at $M = 1.37$ their values are about one-half of those at $M = 1.03$.

Neither model 2 nor 3 (which had the 1.78-percent-thick wings) showed any indication of wing flutter over any portion of the test Mach number range.

CONCLUSIONS

Flight tests to determine the effect of thin externally braced wings on drag near zero lift indicate the following conclusions:

1. When the wing thickness was reduced from 4.50 percent to 1.78 percent and external braces above and below the wing were used to supply the bending strength, the total drag coefficient was reduced by about 17 percent at a Mach number of 1.03 and by 7 percent at a Mach number of 1.37.

2. By locating the 1.78-percent-thick wing shoulder high on a rectangular cross-section body and using braces only below the wing, a further reduction in total drag coefficient was achieved. This reduction in total drag coefficient as compared with the 4.50-percent-thick cantilever wing configuration amounted to 31 percent at a Mach number of 1.05 and 15 percent at a Mach number of 1.37.

3. Between Mach numbers of 0.74 and 0.90 the values of drag coefficient for the model with the 4.50-percent-thick cantilever wing and the model with external braces below the 1.78-percent-thick wing were almost the same.

4. The configuration with the 1.78-percent-thick wing and external braces below the wing had a later drag rise Mach number than the one having the 4.50-percent-thick cantilever wing.

5. Neither of the 1.78-percent-thick wings with external bracing showed any indication of flutter over any portion of the test Mach number range.

Langley Aeronautical Laboratory,
National Advisory Committee for Aeronautics,
Langley Field, Va., June 19, 1957.

REFERENCES

1. Schult, Eugene D.: Large-Scale Flight Measurements of Zero-Lift Drag at Mach Numbers From 0.8 to 1.6 of a Wing-Body Combination Having an Unswept 4.5-Percent-Thick Wing With Modified Hexagonal Sections. NACA RM L51A15, 1951.

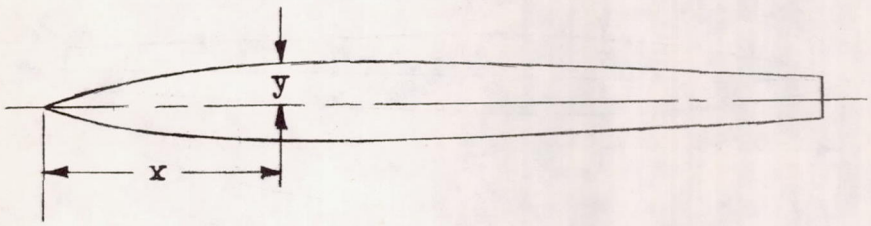
2. Wallskog, Harvey A., and Hart, Roger G.: Investigation of the Drag of Blunt-Nosed Bodies of Revolution in Free Flight at Mach Numbers From 0.6 to 2.3. NACA RM L53D14a, 1953.

3. Ladson, Charles L.: Two-Dimensional Airfoil Characteristics of Four NACA 6A-Series Airfoils at Transonic Mach Numbers Up to 1.25. NACA RM L57F05, 1957.

TABLE I

BODY COORDINATES OF MODEL 1

[Body coordinates are in inches.]

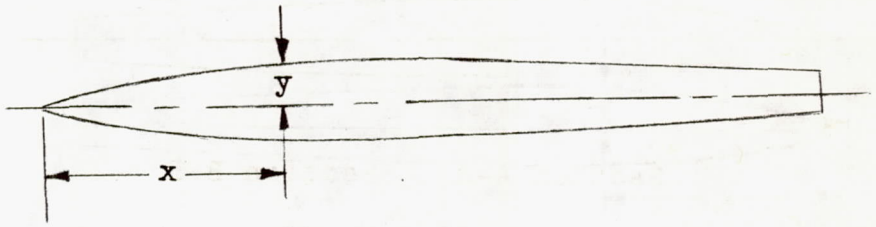


x	y
0.00	0.000
.78	.194
1.17	.289
1.95	.478
3.90	.938
7.80	1.804
11.70	2.596
15.60	3.315
23.40	4.534
31.20	5.460
39.00	6.094
46.80	6.435
54.60	6.496
62.40	6.442
70.20	6.322
78.00	6.137
85.50	5.886
93.60	5.570
101.40	5.188
109.20	4.742
117.00	4.229
124.80	3.652
130.00	3.230

TABLE II

BODY COORDINATES OF MODEL 2

[Body coordinates are in inches.]

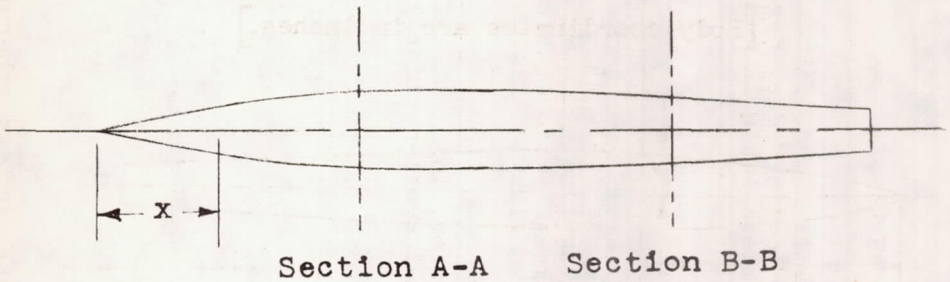


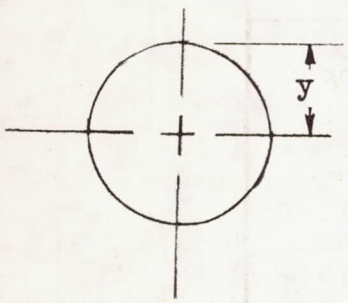
x	y
0.00	0.000
1.00	.186
2.00	.481
4.00	.923
6.00	1.325
7.00	1.510
8.00	1.691
10.00	2.018
14.00	2.558
18.00	2.940
20.00	3.075
22.00	3.173
26.00	3.245
30.00	3.238
34.00	3.185
38.00	3.095
40.00	3.041
42.00	2.979
45.00	2.864
48.00	2.733
50.00	2.637
52.00	2.524
56.00	2.289
60.00	2.019
64.00	1.710
65.00	1.628

TABLE III

BODY COORDINATES OF MODEL 3

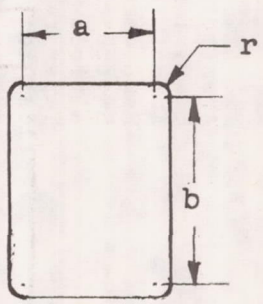
[Body coordinates are in inches.]





Section A-A

Typical cross section between
x = 0 and x = 7.63
($A = \pi y^2$)

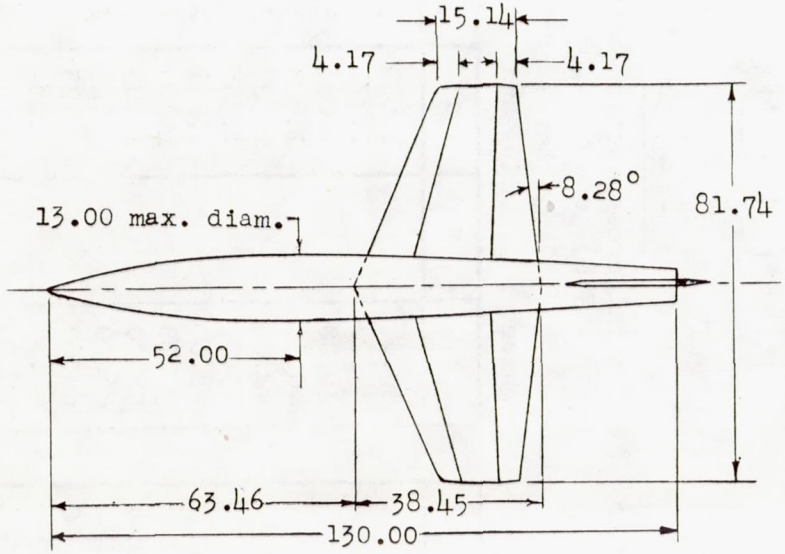


Section B-B

Typical cross section between
x = 7.63 and x = 65.00
($A = 2a^2 + 6ar + \pi r^2$)
where r = 1.625 and b = 2a

x	y	a	b
0.00	0.000		
1.00	.245		
2.00	.480		
4.00	.922		
6.00	1.325		
7.00	1.512		
7.63	1.625		
8.00		0.068	0.136
10.00		.422	.844
14.00		1.032	2.064
18.00		1.480	2.960
20.00		1.639	3.278
22.00		1.753	3.506
26.00		1.851	3.702

x	y	a	b
30.00		1.830	3.660
34.00		1.776	3.552
38.00		1.668	3.336
40.00		1.603	3.206
42.00		1.527	3.054
45.00		1.395	2.790
48.00		1.241	2.482
50.00		1.127	2.254
52.00		1.003	2.006
56.00		.729	1.458
60.00		.423	.846
64.00		.089	.178
65.00	1.625		



PHYSICAL CHARACTERISTICS OF MODEL 1

Wing:	
Area(total), sq ft	15.26
Span, ft	6.80
Aspect ratio	3.04
Mean aerodynamic chord, ft	2.38
Sweepback of leading edge, deg	23.03
Airfoil thickness ratio	0.045
Taper ratio	0.39
Vertical tail:	
Area(total), sq ft	1.89
Span, ft	3.04
Aspect ratio	4.88
Airfoil thickness ratio at model center line	0.018
Airfoil thickness ratio at tip	0.042
Taper ratio	0.42
Body:	
Length, in.	130.00
Maximum diameter, in.	13.00
Maximum normal cross-sectional area, sq in.	132.8

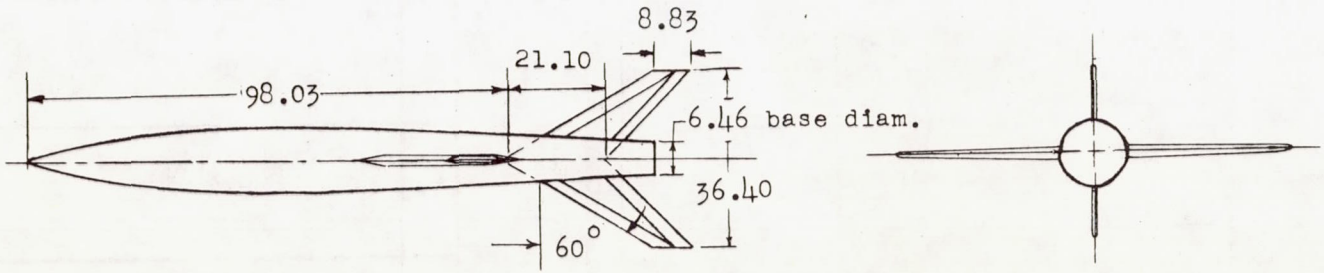
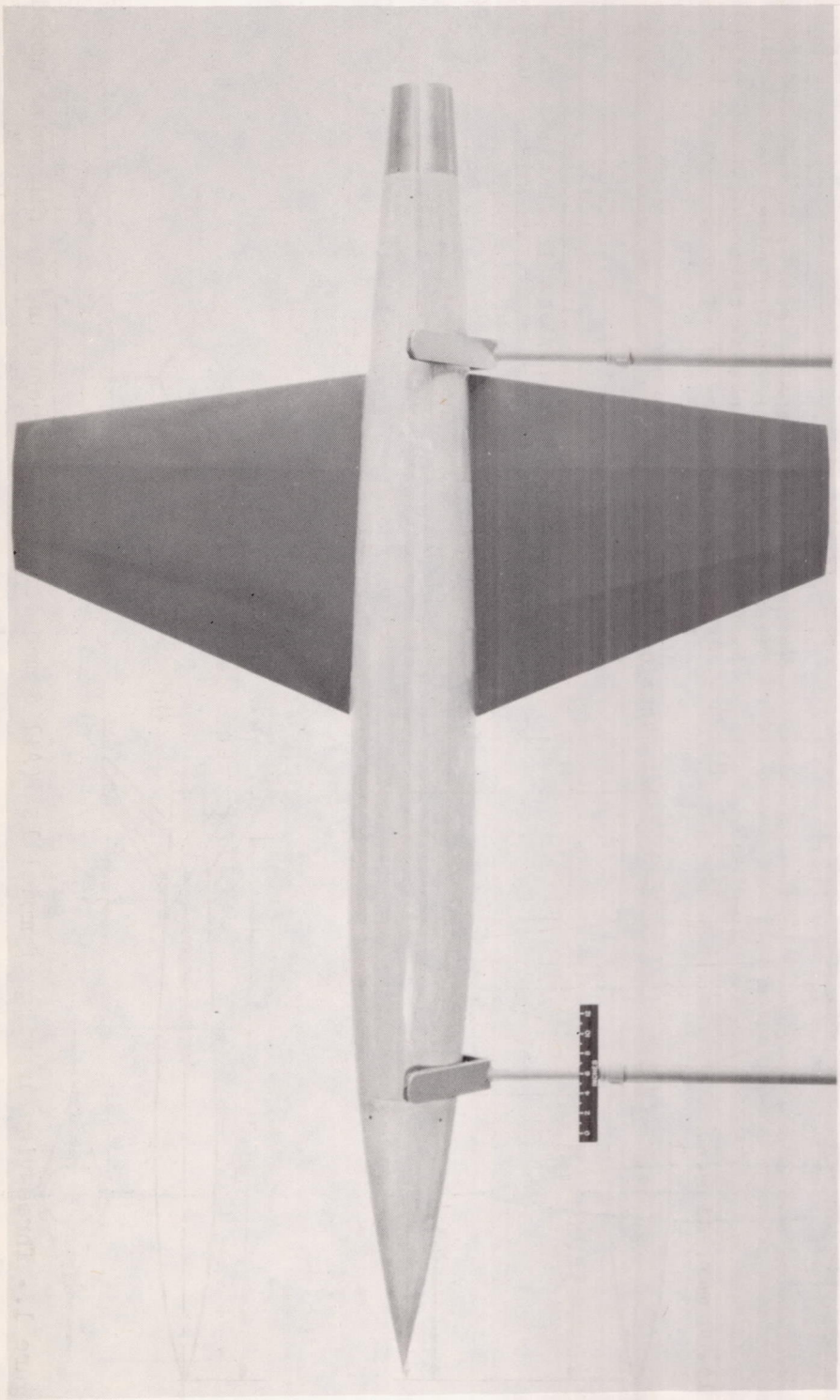


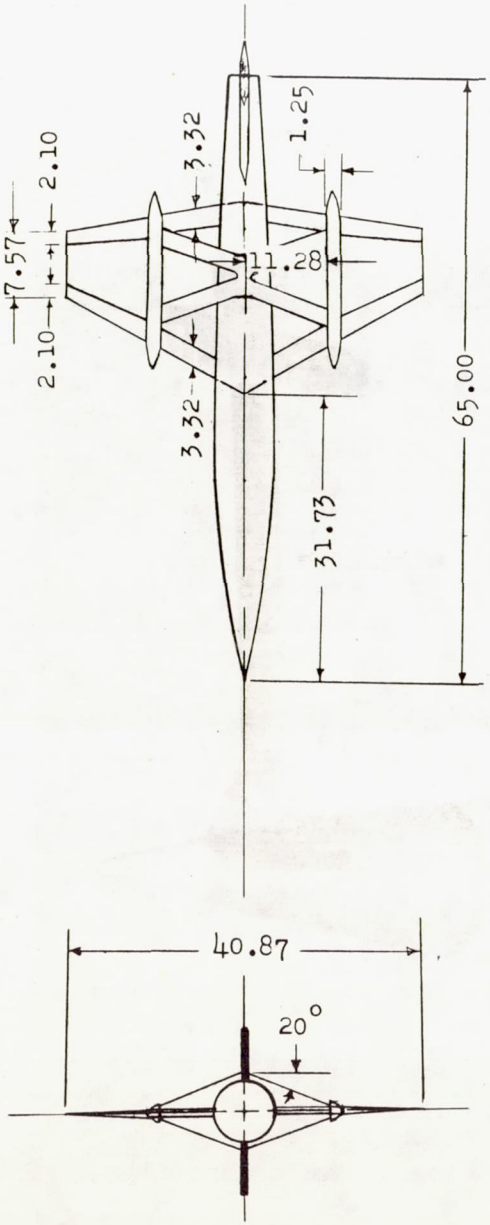
Figure 1.- Three-view drawing of model 1. (All dimensions are in inches unless otherwise noted.)

CONFIDENTIAL



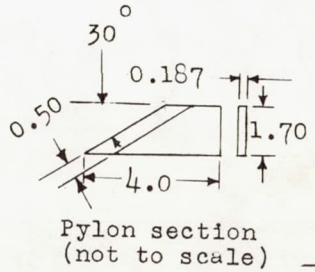
L-65864.1

Figure 2.- Model 1.



PHYSICAL CHARACTERISTICS OF MODEL 2

Wing:	
Area(total), sq ft	3.82
Span, ft	3.40
Aspect ratio	3.04
Mean aerodynamic chord, ft	1.19
Sweepback of leading edge, deg	23.03
Airfoil thickness ratio at root	0.013
Airfoil thickness ratio at pod	0.020
Airfoil thickness ratio at tip	0.020
Taper ratio	0.39
Vertical tail:	
Area(total), sq ft	0.47
Span, ft	1.52
Aspect ratio	4.88
Airfoil thickness ratio at model center line	0.018
Airfoil thickness ratio at tip	0.042
Taper ratio	0.42
Body:	
Length, in.	65.00
Maximum diameter, in.	6.50
Maximum normal cross-sectional area, sq in.	33.2



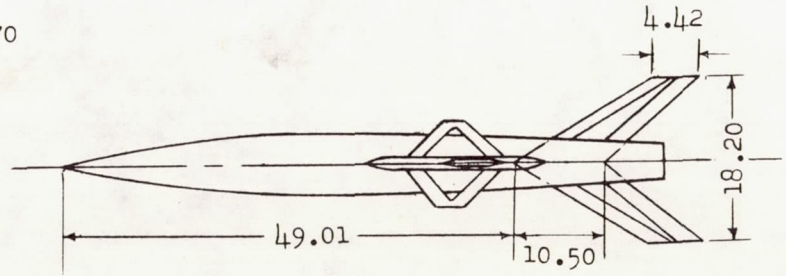
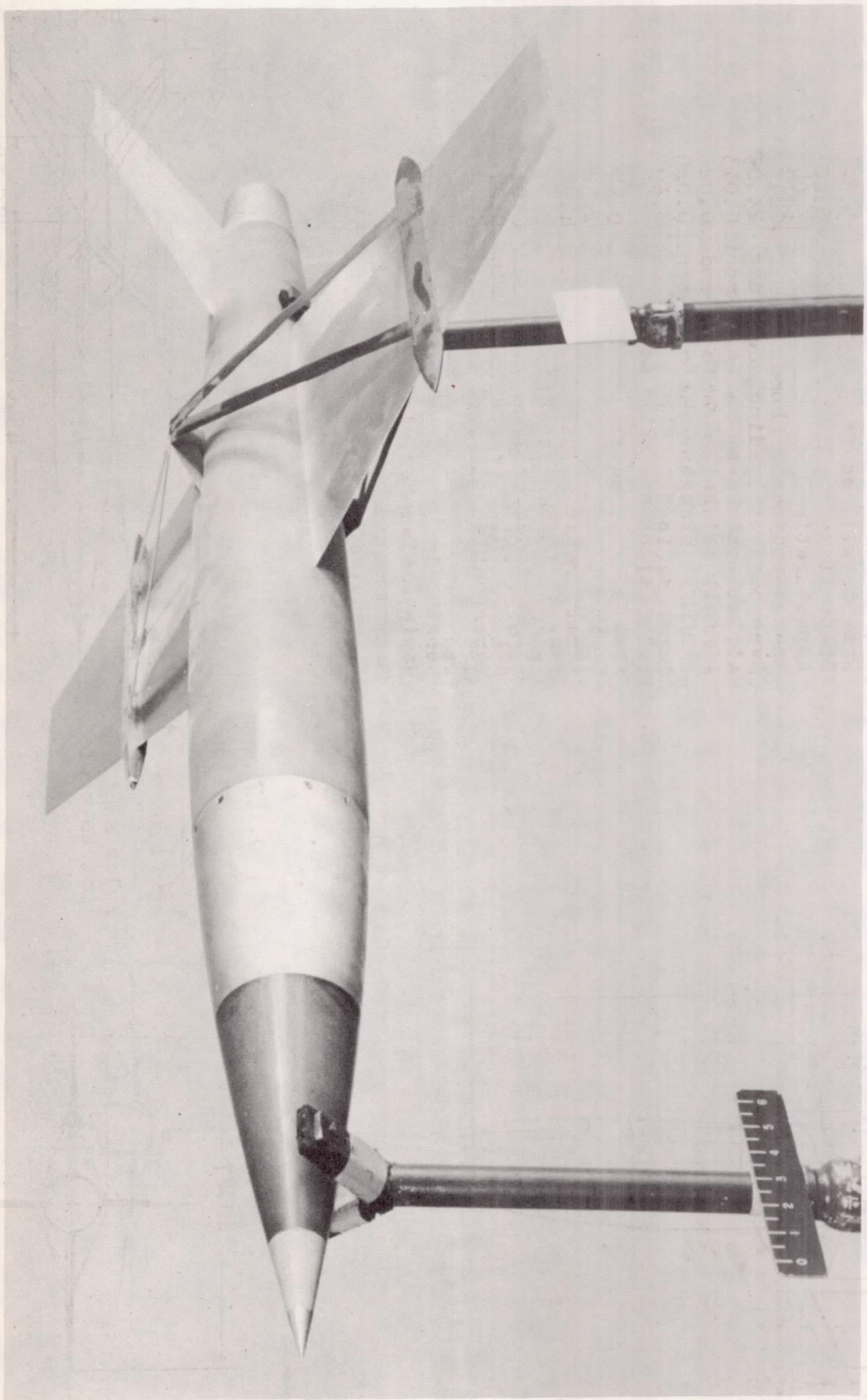
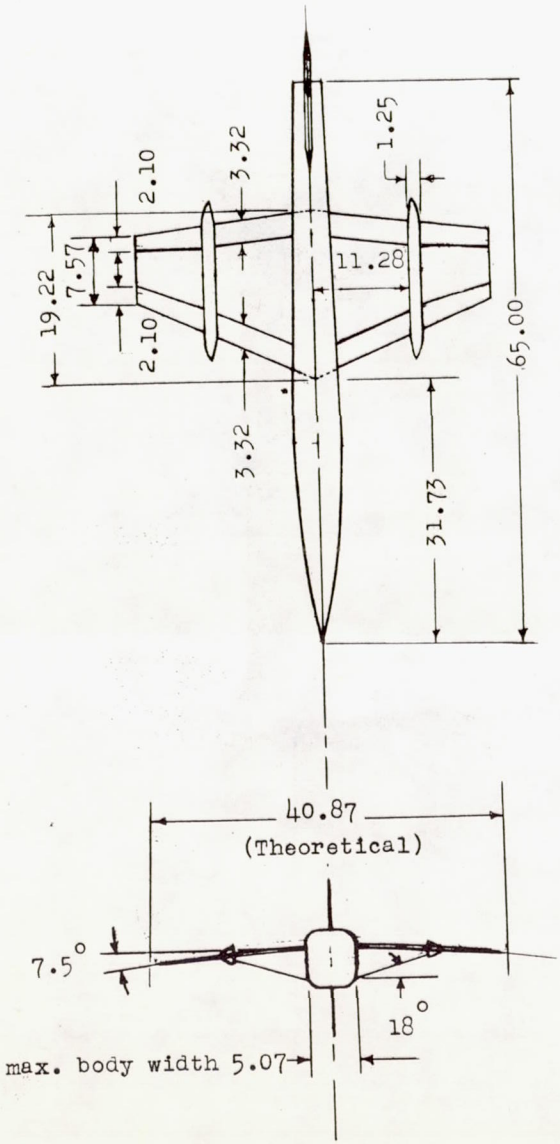


Figure 3.- Three-view drawing of model 2. (All dimensions are in inches unless otherwise noted.)



L-86777.1

Figure 4.- Model 2.



PHYSICAL CHARACTERISTICS OF MODEL 3

Wing:	
Area(total), sq ft	3.82
Span, ft	3.40
Aspect ratio	3.04
Mean aerodynamic chord, ft	1.19
Sweepback of leading edge, deg	23.03
Airfoil thickness ratio at root	0.013
Airfoil thickness ratio at pod	0.020
Airfoil thickness ratio at tip	0.020
Taper ratio	0.39
Vertical tail:	
Area(total), sq ft	0.47
Span, ft	1.52
Aspect ratio	4.88
Airfoil thickness ratio at model center line	0.018
Airfoil thickness ratio at tip	0.042
Taper ratio	0.42
Body:	
Length, in.	65.00
Maximum normal cross-sectional area, sq in.	33.20

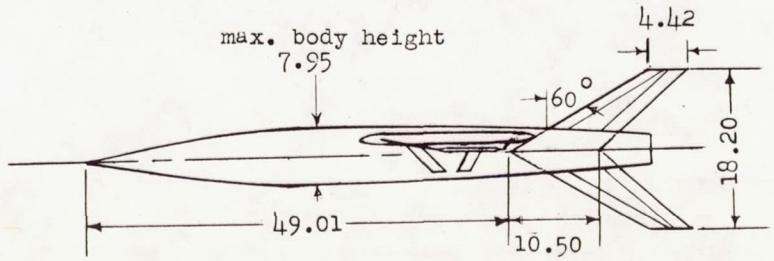
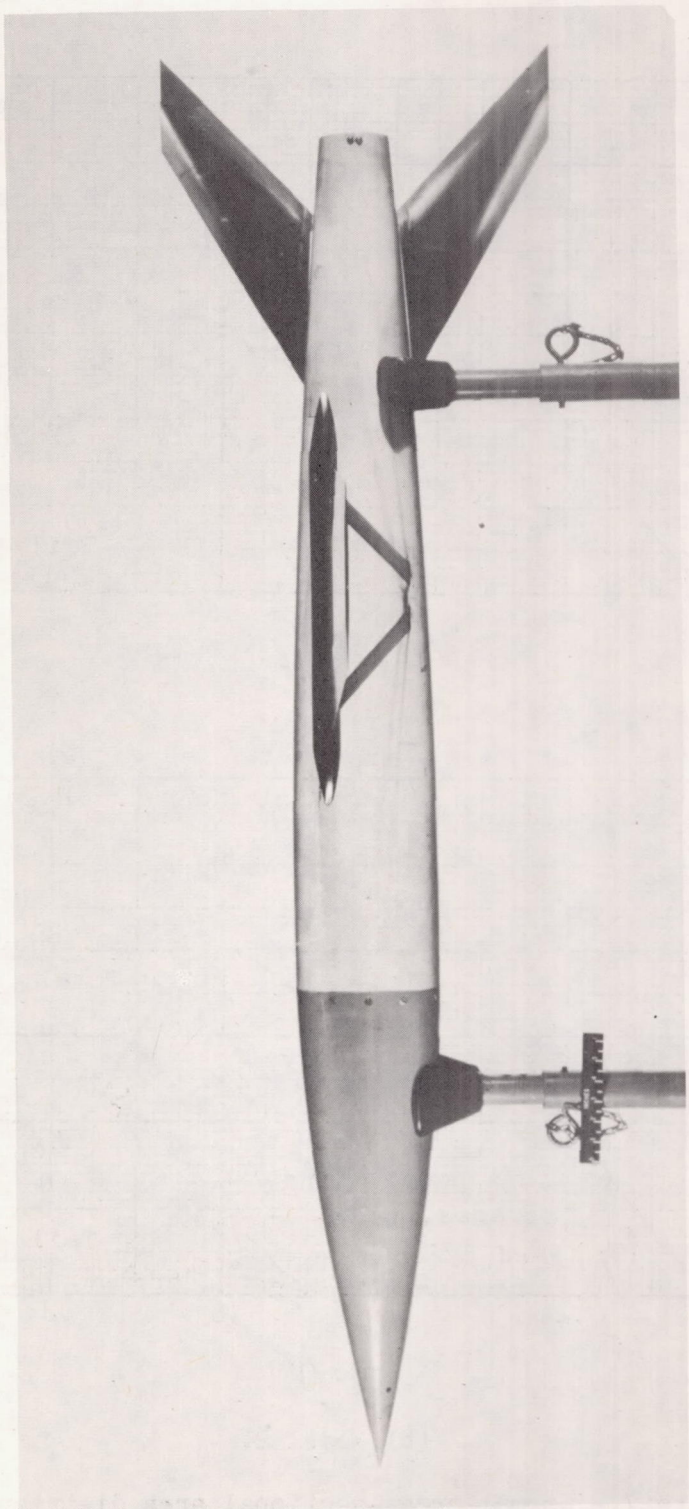
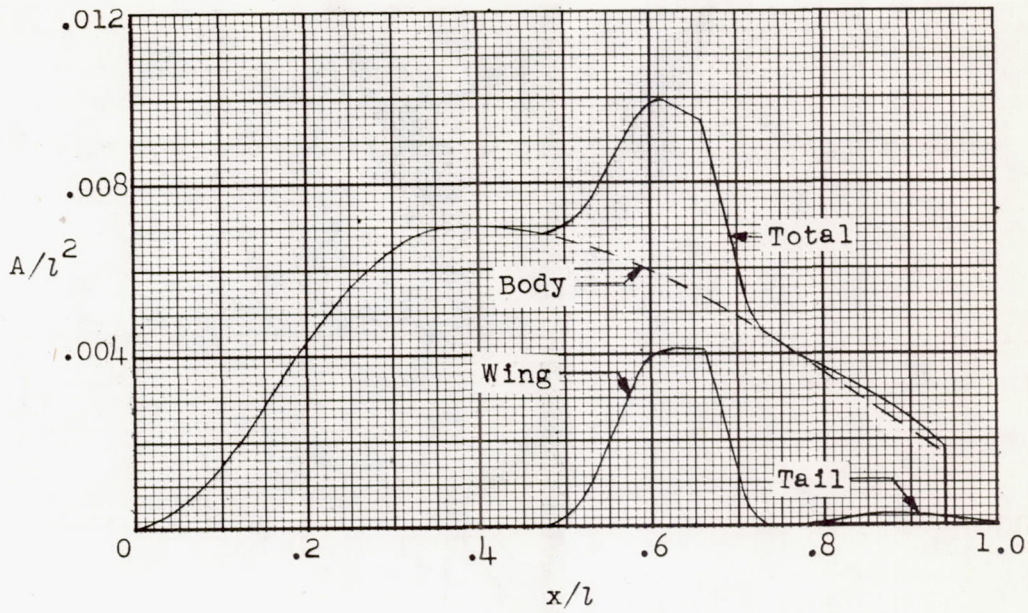


Figure 5.- Three-view drawing of model 3. (All dimensions are in inches unless otherwise noted.)

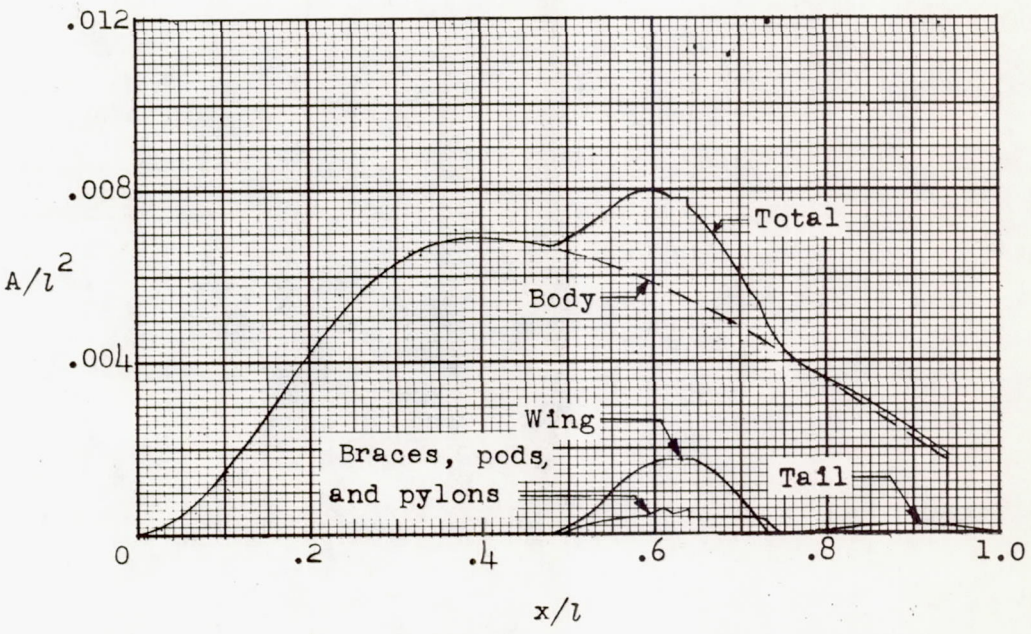


L-96661

Figure 6.- Model 3.

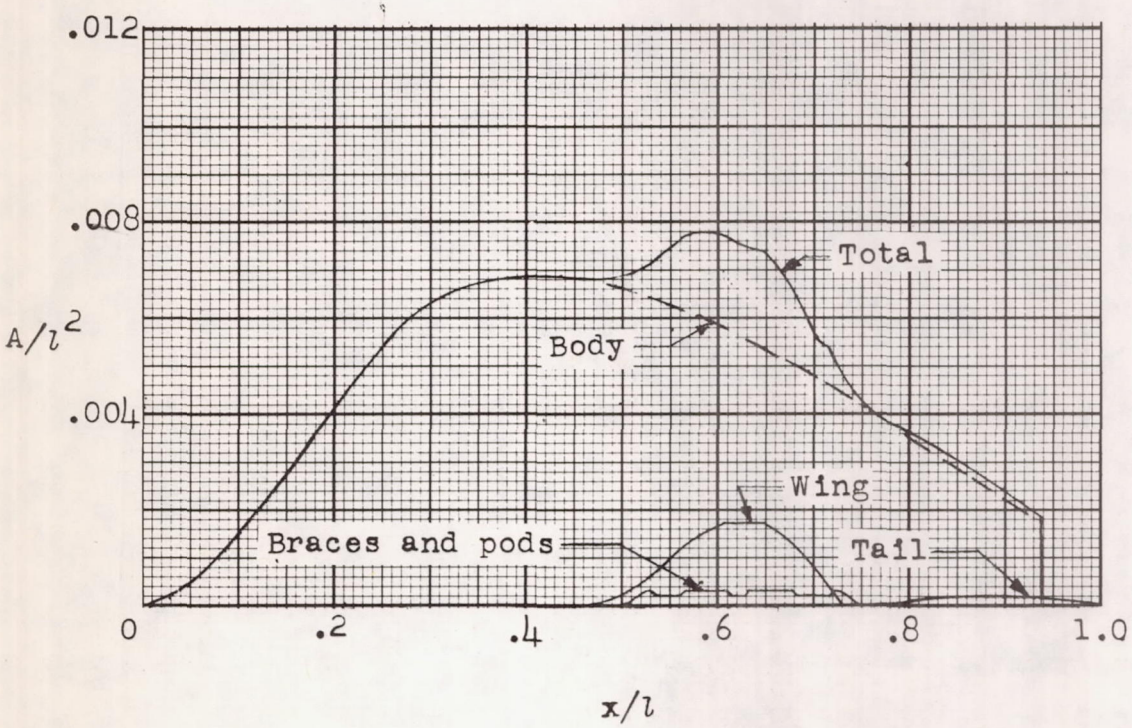


(a) Model 1.



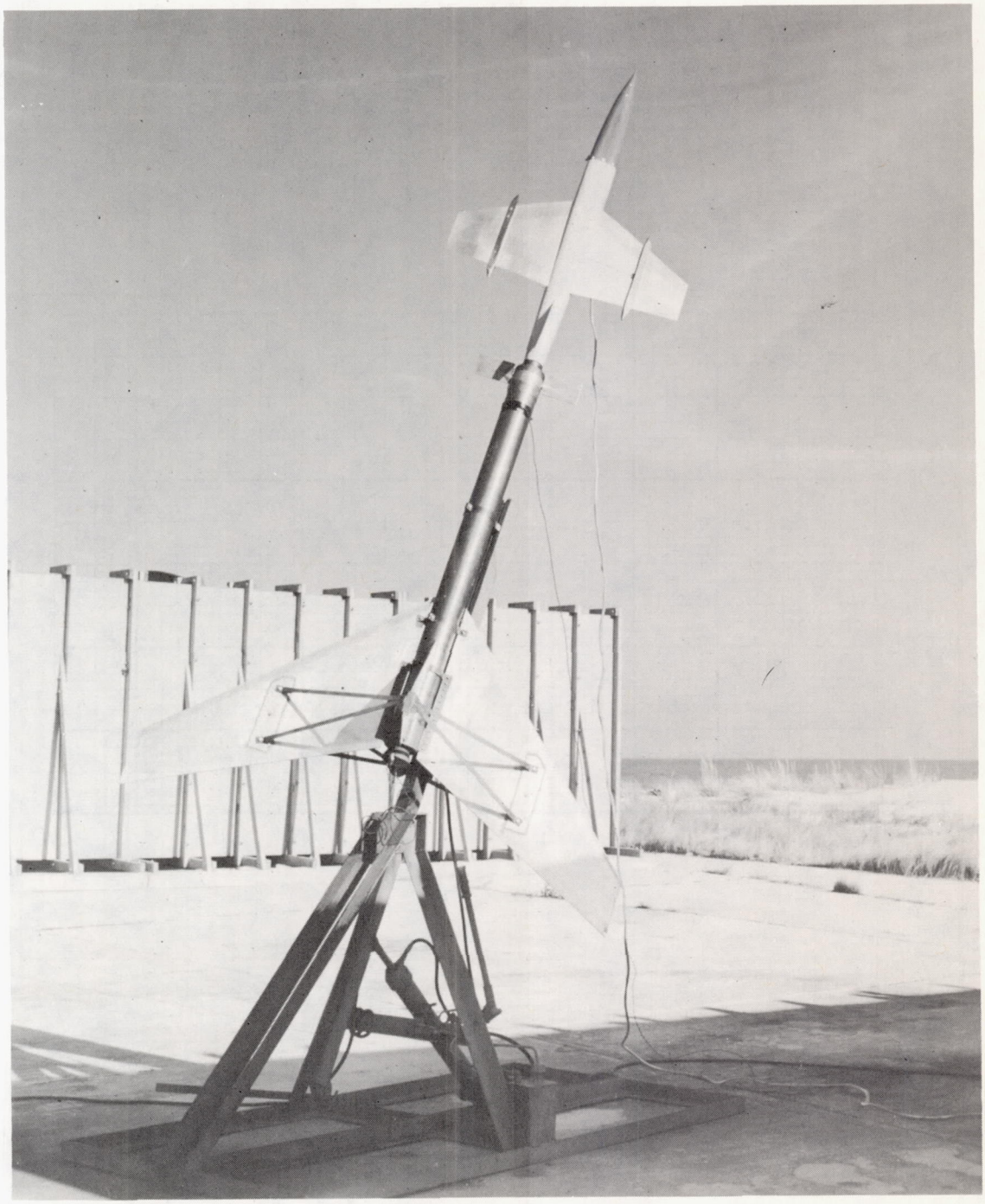
(b) Model 2.

Figure 7.- Normal cross-sectional area distribution.



(c) Model 3.

Figure 7.- Concluded.



L-96976.1

Figure 8.- Typical model-booster combination prior to launching.

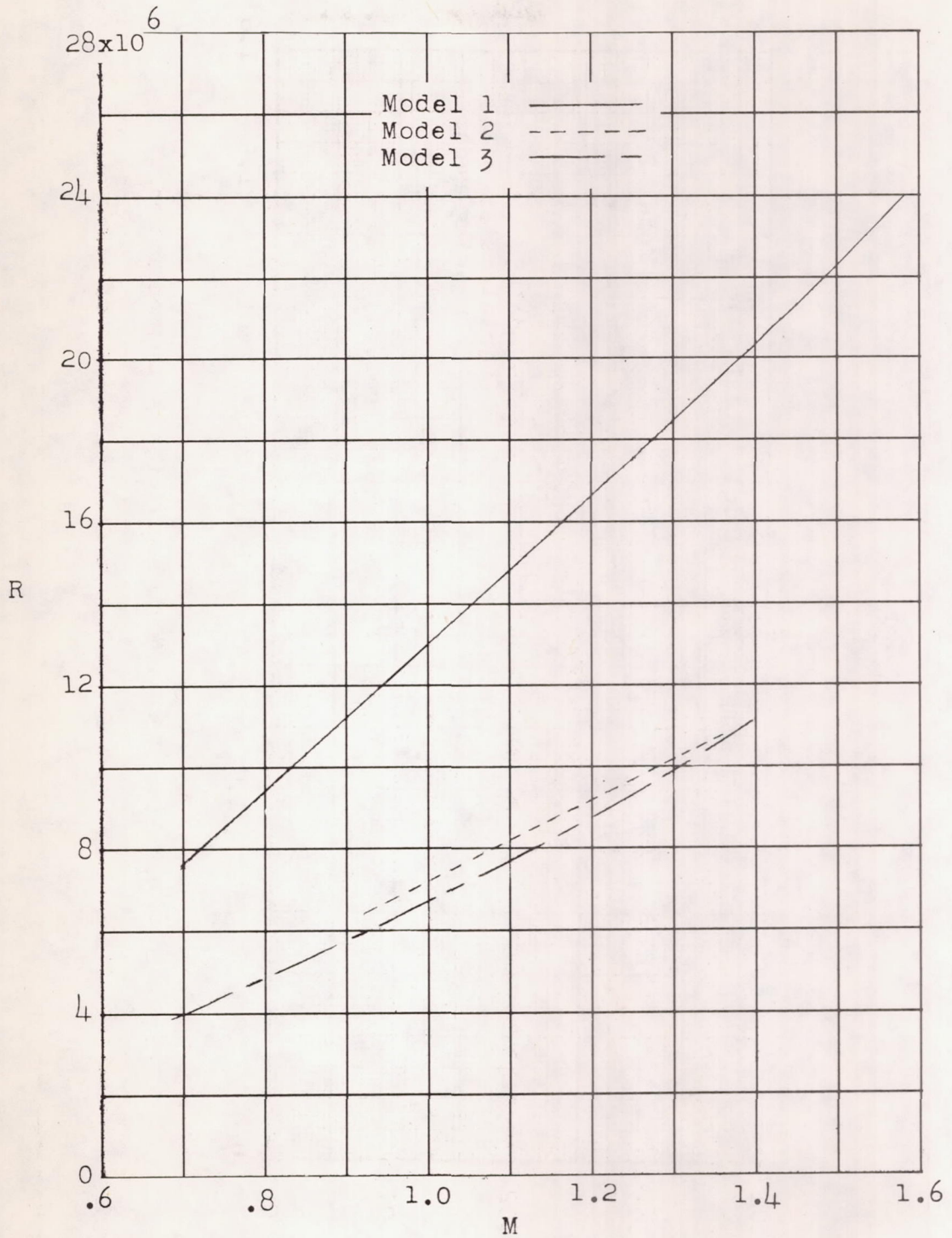


Figure 9.- Variation of Reynolds number based on length of mean aerodynamic chord with Mach number for three models.

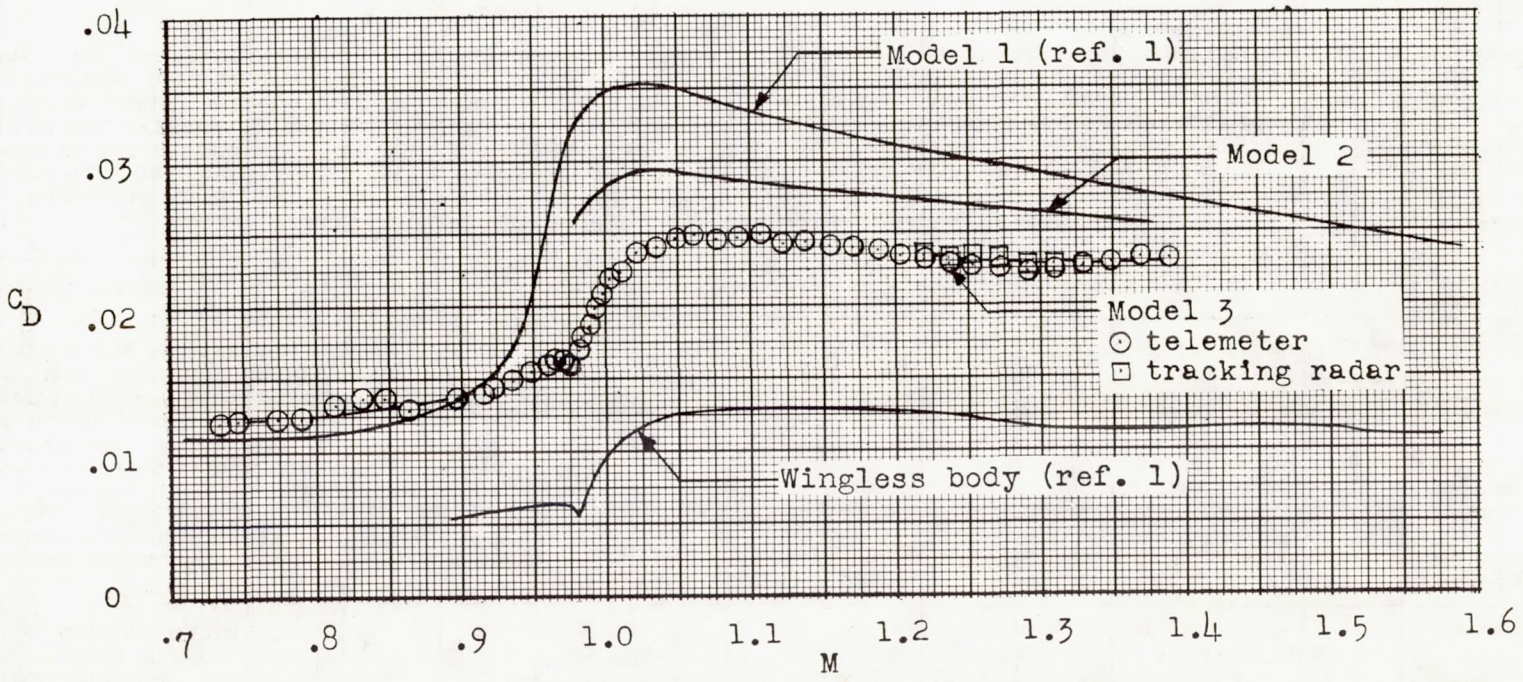


Figure 10.- Variation of total drag coefficient with Mach number.

NACA - Langley Field, Va.